Numerical solution of nonlinear time-fractional Cable equation by finite volume element method

A. Yazdani
Department of Mathematics
University of Mazandaran
Babolsar
Iran
yazdani@umz.ac.ir

R. Yousefian*
Department of Mathematics
University of Mazandaran
Babolsar
Iran
r.yousefian@stu.umz.ac.ir

Abstract. In this paper, we study the use of finite volume element method and see how we can employ finite element bases to numerical solution of nonlinear time fractional Cable equation in one dimension. Finite element bases are as linear polynomials which are compactly supported. Caputo in the proposed scheme constitutes the fractional derivative. This scheme will be analyzed and the stability of the method will be discussed. Furthermore, the numerical results are compared with analytical solution to ascertain how accurate the presented method is.

Keywords: finite volume element method, nonlinear systems, Cable equation, Caputo derivative, Von-Neumann stability analysis.

1. Introduction

In this paper, the nonlinear fractional Cable equation is denoted:

$$(1) \quad \begin{cases} u_t +_0^C D_t^{\vartheta} u(x,t) -_0^C D_t^{\vartheta} u_{xx}(x,t) + f(u) = s(x,t), & \text{in } I \times (0,T], \\ u(0,t) = g_1(t), & t \in (0,T], \\ u(1,t) = g_2(t), & t \in (0,T], \\ u(x,0) = u_0(x), & \text{in } I. \end{cases}$$

In $0 < \vartheta < 1$ and $I = (0,1)$ be the computational domain $s(x,t)$, where $s(x,t)$ is a continuous function, that we define as source term. Let subscripts x and t are the space and time differentiations, respectively, and superscript ϑ is the order of fractional derivative. Here the fractional derivatives is in the Caputo

∗. Corresponding author

sense [6], i.e.

$$\frac{\partial^{\vartheta} u(x,t)}{\partial t^{\vartheta}} = \frac{1}{\Gamma(1-\vartheta)} \int_0^t \frac{\partial u(x,\xi)}{\partial \xi} \frac{d\xi}{(t-\xi)^{\vartheta}}, \qquad 0 < \vartheta < 1 \tag{2}$$

in which $\Gamma(\vartheta)$ is the Gamma function.

Different initial-boundary value problems including Cable equation, have been solved analytically by many authors [9, 8, 7, 2, 3].

In this paper, the time fractional Cable equation is considered as an initial-boundary value problem to solve it numerically. The scheme illustrated here is finite difference method to discretize the time fractional derivative, along with finite volume element method with linear B-spline basis function to discretize in space scale. The time fractional derivative is in the Caputo sense, and will discretize by a backward finite difference formula. The resulting proposed scheme will be shown to be unconditionally stable.

This paper is outlined as follows. In Section 2, the numerical method is described. In Section 3, the stability of the scheme is investigated. In Section 4, the recommended scheme is demonstrated with the help of some numerical test examples, and in the end, Section 5 provides us with conclusions.

2. Finite volume element method

The finite volume element method (FVEM), which in fact is a variation of the finite volume method (FVM), is also regarded as a Petrov-Galerkin finite element method (FEM).

Here, we can denote some preliminaries around FVEM and Sobolev spaces.

Let $I = (a, b) \subset \mathbf{R}$ be a domain, we will employ the standard notation for Sobolev spaces $H^s(I), s \geq 0$, making up functions v which include generalized derivatives of order s in the spaces $L_2(I)$ for all $|\alpha| \leq s$. The norm and seminorm of $H^s(I)$ are defined by

$$\|v\|_s = (\sum_{|\alpha|\leq s} |D^{\alpha} v|^2)^{\frac{1}{2}}, \qquad |v|_s = (\sum_{|\alpha|=s} |D^{\alpha} v|^2)^{\frac{1}{2}}.$$

Parallel with the Sobolev space $H^s(I)$, we have the space $H_0^1(I)$ the subspace of $H^1(I)$ which include functions that disappear on the boundary of I, i.e.,

$$H_0^1(I) = \{v \in H^1(I), I = [a, b], v|_{\partial I} = 0\}.$$

To clarify the proposed numerical method [1], let's focus on the equation (1). We divide the domain I into finite elements $I_i = [x_{i-1}, x_i]$ with the nodes $x_i, i = 0, 1, 2, ..., M$ and set $h_i = x_i - x_{i-1}$. Let a primal partition of I with elements I_i denotes by $\zeta_h : a = x_0 < x_1 < x_2 < ... < x_M = b$. Set element $I_i = [x_{i-1}, x_i]$, midpoint $x_{i-\frac{1}{2}} = (x_i + x_{i-1})/2$. Let $I_0^* = [0, x_{\frac{1}{2}}]$, $I_i^* = [x_{i-\frac{1}{2}}, x_{i+\frac{1}{2}}](i = 1, ..., M-1)$ and $I_M^* = [x_{M-\frac{1}{2}}, 1]$ compose the dual partition ζ_i^* of ζ_i. All $I_i^*(i = 0, 1, 2, ..., M)$ called control volumes.

Consider the trial and test spaces S_h as the linear element space with basis functions at the point x_i

$$\phi_i(x) = \begin{cases} \dfrac{x - x_{i-1}}{h_i}, & x_{i-1} \le x \le x_i, \\ \dfrac{x_{i+1} - x}{h_{i+1}}, & x_i \le x \le x_{i+1}, \qquad 1 \le i \le M-1 \\ 0, & \text{otherwise}, \end{cases} \tag{3}$$

and

$$\phi_0(x) = \begin{cases} \dfrac{x - x_1}{x_0 - x_1}, & x_0 \le x \le x_1, \\ 0, & \text{otherwise}, \end{cases},$$
$$\phi_M(x) = \begin{cases} \dfrac{x - x_{M-1}}{x_M - x_{M-1}}, & x_{M-1} \le x \le x_M, \\ 0, & \text{otherwise}, \end{cases} \tag{4}$$

and S_h^* as piecewise constant function space with basis function of the point x_i

$$\chi_i(x_j) = \begin{cases} 1, & x_j \in I_i^*, \\ 0, & \text{otherwise}. \end{cases} \tag{5}$$

The choise of different solution spaces, test spaces, and dual partitions leads to different FVE methods [4].

The linear basis functions $\phi_i(x)$ and their first derivatives vanish outside the interval $[x_{i-1}, x_{i+1}]$. We can observe the values of $\phi_i(x)$ and its first derivative $\phi_i'(x)$ at the knots in Table 1.

Table 1: Quantities of basis functions and their first derivatives in points $x_{i-\frac{1}{2}}$ and $x_{i+\frac{1}{2}}$.

	$x_{i-\frac{1}{2}}$	$x_{i+\frac{1}{2}}$		$x_{i-\frac{1}{2}}$	$x_{i+\frac{1}{2}}$
ϕ_{i-1}	$\frac{1}{2}$	0	ϕ_{i-1}'	$\frac{1}{h}$	0
ϕ_i	$\frac{1}{2}$	$\frac{1}{2}$	ϕ_i'	$\frac{1}{h}$	$-\frac{1}{h}$
ϕ_{i+1}	0	$\frac{1}{2}$	ϕ_{i+1}'	0	$-\frac{1}{h}$

The standard Lagrangian interpolation operator is also defined

$$I_h : C(I) \to S_h, \qquad s.t. \qquad I_h u = \sum_{i=0}^{M} u_i \phi_i(x), \qquad \forall u \in C(I), \tag{6}$$

$$I_h^* : C(I) \to S_h^*, \qquad s.t. \qquad I_h^* u = \sum_{i=0}^{M} u_i \chi_i(x), \qquad \forall u \in C(I), \tag{7}$$

where $u_i = u(x_i)$.

Regarding basis functions ϕ_i, each $u_h(x,t) \in S_h$ may be written as

$$u_h(x,t) = \sum_{i=0}^{M} \delta_i(t)\phi_i(x), \qquad t > 0, \tag{8}$$

where the time-dependent coefficients $\delta_i(t)$ are unknown and, with the help of the finite volume element method, we can compute them from the initial and boundary conditions.

Afterwards, we can define the FVE approximation u_h of (1) as a solution to the following problem: Find $u_h \in S_h$, for each $t > 0$, such that for all control volume $I_i^*, i = 0, 1, 2, ..., M$

$$(\frac{\partial u_h}{\partial t}, I_h^* v_h) + (\frac{\partial^\vartheta u_h}{\partial t^\vartheta}, I_h^* v_h) + a(u_h, I_h^* v_h) = (s, I_h^* v_h), \qquad I_h^* \in S_h, \tag{9}$$

We here define the bilinear form $a(u_h, I_h^* v_h)$ as follows:

$$a(u_h, I_h^* v_h) = (I_h f(u_h), I_h^* v_h) - (\frac{\partial^\vartheta (u_h)_{xx}}{\partial t^\vartheta}, I_h^* v_h),$$

where $(.,.)$ is inner product in $L_2(I)$ and $f(u) = u^2$.

Explaining the FVE method for problem (1), we can verify that

$$\int_I \frac{\partial u_h}{\partial t}\chi_i dx + \int_I \frac{\partial^\vartheta u_h}{\partial t^\vartheta}\chi_i dx + \int_I I_h(u_h)^2 \chi_i dx - \int_I \frac{\partial^\vartheta (u_h)_{xx}}{\partial t^\vartheta}\chi_i dx$$
$$= \int_I s\chi_i dx, \qquad i = 0, 1, 2, ..., M.$$

According to definition of χ_i, $i = 0, 1, 2, ..., M$, we have

$$\int_{I_i^*} \frac{\partial u_h}{\partial t} dx + \int_{I_i^*} \frac{\partial^\vartheta u_h}{\partial t^\vartheta} dx + \int_{I_i^*} I_h(u_h)^2 dx - \int_{I_i^*} \frac{\partial^\vartheta (u_h)_{xx}}{\partial t^\vartheta} dx$$
$$= \int_{I_i^*} s dx, \qquad i = 0, 1, 2, ..., M. \tag{10}$$

Let $\delta_i = \delta_i(t)$, $\delta_i^{(\vartheta)} = \frac{\partial^\vartheta \delta_i(t)}{\partial t^\vartheta}$ and $f_i(t) = f(u_h(x_i, t))$. If we apply (8) to every control volume l_i^* and use (2) and Table 1, we have

$$\int_{I_i^*} \frac{\partial u_h}{\partial t} dx = \frac{h}{8}\{\delta_{i-1}' + 6\delta_i' + \delta_{i+1}'\}, \tag{11}$$

and

$$\int_{I_i^*} \frac{\partial^\vartheta u_h}{\partial t^\vartheta} dx = \frac{h}{8}\{\delta_{i-1}^\vartheta + 6\delta_i^\vartheta + \delta_{i+1}^\vartheta\}, \tag{12}$$

and

$$\int_{I_i^*} \frac{\partial^\vartheta (u_h)_{xx}}{\partial t^\vartheta} dx = \frac{1}{h}\{\delta_{i-1}^\vartheta - 2\delta_i^\vartheta + \delta_{i+1}^\vartheta\}, \tag{13}$$

and

$$\int_{I_i^*} I_h(u_h)^2 dx = \frac{h}{24}\{\delta_{i-1}^2 + 14\delta_i^2 + \delta_{i+1}^2\}. \tag{14}$$

If we substitute (11), (12), (13) and (14) in (10), we can reach the semi-discrete form of (10) as a formula we see below

$$\begin{aligned} &\frac{h}{8}\{(\delta_{i-1}^{'} + \delta_{i-1}^\vartheta) + 6(\delta_i^{'} + \delta_i^\vartheta) + (\delta_{i+1}^{'} + \delta_{i+1}^\vartheta)\} \\ &+ \frac{h}{24}\{\delta_{i-1}^2 + 14\delta_i^2 + \delta_{i+1}^2\} - \frac{1}{h}\{\delta_{i-1}^\vartheta - 2\delta_i^\vartheta + \delta_{i+1}^\vartheta\} \\ &= \int_{I_i^*} s dx, \qquad i = 1, 2, ..., M-1. \end{aligned} \tag{15}$$

We have also for I_0^* and I_M^*, respectively,

$$\begin{aligned} &\frac{3h}{8}(\delta_0^{'} + \delta_0^{(\vartheta)}) + \frac{h}{8}(\delta_1^{'} + \delta_1^{(\vartheta)}) + \frac{h}{24}\{7\delta_0^2 + \delta_1^2\} - \frac{1}{h}\{\delta_1^\vartheta - \delta_0^\vartheta\} = \int_{I_i^*} s dx, \\ &\frac{h}{8}(\delta_{M-1}^{'} + \delta_{M-1}^{(\vartheta)}) + \frac{3h}{8}(\delta_M^{'} + \delta_M^{(\vartheta)}) + \frac{h}{24}\{7\delta_M^2 + \delta_{M-1}^2\} - \frac{1}{h}\{\delta_{M-1}^\vartheta - \delta_M^\vartheta\} \\ &= \int_{I_M^*} s dx. \end{aligned} \tag{16}$$

We define $\Delta t = \tau = t_k - t_{k-1}, k = 1, 2, ..., n, t_k = k\tau$ and $x_i = ih, i = 0, 1, ..., M$ where τ and h are time and space steps, respectively. We can consider $\delta_i^k := u_h(x_i, t_k)$ as the approximation value of $u(x_i, t_k)$ by FVEM.

The time fractional derivative is discretized with the help of the Caputo derivative formulation for $\delta_i^{(\vartheta)}(t)$, as seen below

$$\begin{aligned} \frac{\partial^\vartheta \delta_i(t_{k+1})}{\partial t^\vartheta} &= \frac{1}{\Gamma(1-\vartheta)} \sum_{j=0}^{k} \int_{t_j}^{t_{j+1}} (t_{k+1} - \xi)^{-\vartheta} \frac{\partial \delta(x_i, \xi)}{\partial \xi} d\xi \\ &\simeq \frac{1}{\Gamma(1-\vartheta)} \sum_{j=0}^{k} \frac{1}{\tau}[\delta(x_i, t_{j+1}) - \delta(x_i, t_j)] \int_{t_j}^{t_{j+1}} (t_{k+1} - \xi)^{-\vartheta} d\xi \\ &= \frac{1}{(1-\vartheta)\Gamma(1-\vartheta)\tau^\vartheta} \sum_{j=0}^{k} \Theta_{k-j}[\delta(x_i, t_{j+1}) - \delta(x_i, t_j)] \\ &= \psi_{\vartheta,\tau} \sum_{s=0}^{k} \Theta_s[\delta_i^{k-s+1} - \delta_i^{k-s}], \end{aligned} \tag{17}$$

where $\psi_{\vartheta,\tau} = \frac{\tau^{-\vartheta}}{\Gamma(2-\vartheta)}$ and $\Theta_s = (s+1)^{1-\vartheta} - s^{1-\vartheta}, s = 0, 1, ..., n$.

Truncation error of the approximation (17) is denoted by

$$R_\tau^{k+1} := \frac{\partial^\vartheta \delta_i(t_{k+1})}{\partial t^\vartheta} - \psi_{\vartheta,\tau} \sum_{s=0}^{k} \Theta_s [\delta_i^{k-s+1} - \delta_i^{k-s}], \tag{18}$$

and we have [5]

$$R_\tau^{k+1} \le C_u \tau^{2-\vartheta}, \tag{19}$$

in which C_u is a constant only related to u.

Lemma 1 ([7])**.** For coefficients Θ_s, we have

1. $\Theta_0 = 1$,
2. $\Theta_s > 0, \qquad s = 0, 1, ..., n$,
3. $\Theta_s > \Theta_{s+1}, \qquad s = 0, 1, ..., n-1$.

If we substitute (17) in (15), for a uniform partition $h_i = h$, the fully-discrete formula of the equation (1) can be obtained as the form below

$$\begin{aligned}
&\frac{h}{8\tau}\{(\delta_{i-1}^{k+1} - \delta_{i-1}^{k}) + 6(\delta_i^{k+1} - \delta_i^{k}) + (\delta_{i+1}^{k+1} - \delta_{i+1}^{k})\} \\
&+ r \sum_{s=0}^{k} \Theta_s \{[\delta_{i-1}^{k-s+1} - \delta_{i-1}^{k-s}] - 2[\delta_i^{k-s+1} - \delta_i^{k-s}] + [\delta_{i+1}^{k-s+1} - \delta_{i+1}^{k-s}]\} \\
&- \iota \sum_{s=0}^{k} \Theta_s \{[\delta_{i-1}^{k-s+1} - \delta_{i-1}^{k-s}] + 6[\delta_i^{k-s+1} - \delta_i^{k-s}] + [\delta_{i+1}^{k-s+1} - \delta_{i+1}^{k-s}]\} \\
&+ \frac{h}{24}\{(\delta^2)_{i-1}^{k+1} + 14(\delta^2)_i^{k+1} + (\delta^2)_{i+1}^{k+1}\} = \int_{I_i^*} s(x, t_{k+1}), i = 1, 2, ..., M-1,
\end{aligned} \tag{20}$$

where $r = \frac{h\tau^{-\vartheta}}{8\Gamma(2-\vartheta)}$ and $\iota = \frac{\tau^{-\vartheta}}{h\Gamma(2-\vartheta)}$.

Then, (20) can result in the following recurrence difference formula based on the time-dependent parameters δ_i^k

$$\begin{aligned}
&(\frac{h}{8\tau} + r - \iota)\delta_{i-1}^{k+1} + (\frac{6h}{8\tau} + 6r + 2\iota)\delta_i^{k+1} + (\frac{h}{8\tau} + r - \iota)\delta_{i+1}^{k+1} \\
&+ \frac{h}{24}\{(\delta^2)_{i-1}^{k+1} + 14(\delta^2)_i^{k+1} + (\delta^2)_{i+1}^{k+1}\} \\
&= (\frac{h}{8\tau} + r - \iota)\delta_{i-1}^{k} + (\frac{6h}{8\tau} + 6r + 2\iota)\delta_i^{k} + (\frac{h}{8\tau} + r - \iota)\delta_{i+1}^{k} \\
&+ r \sum_{s=1}^{k} \Theta_s \{[\delta_{i-1}^{k-s+1} - \delta_{i-1}^{k-s}] + 6[\delta_i^{k-s+1} - \delta_i^{k-s}] + [\delta_{i+1}^{k-s+1} - \delta_{i+1}^{k-s}]\} \\
&- \iota \sum_{s=1}^{k} \Theta_s \{[\delta_{i-1}^{k-s+1} - \delta_{i-1}^{k-s}] - 2[\delta_i^{k-s+1} - \delta_i^{k-s}] \\
&+ [\delta_{i+1}^{k-s+1} - \delta_{i+1}^{k-s}]\} + \int_{I_i^*} s(x, t_{k+1}).
\end{aligned} \tag{21}$$

When $k=0$, i.e. in the first temporal step, the scheme simply reads

$$
\begin{aligned}
&(\frac{h}{8\tau}+r-\iota)\delta_{i-1}^1+(\frac{6h}{8\tau}+6r+2\iota)\delta_i^1+(\frac{h}{8\tau}+r-\iota)\delta_{i+1}^1\\
&+\frac{h}{24}\{(\delta^2)_{i-1}^1+14(\delta^2)_i^1+(\delta^2)_{i+1}^1\}=(\frac{h}{8\tau}+r-\iota)\delta_{i-1}^0\\
&+(\frac{6h}{8\tau}+6r+2\iota)\delta_i^0+(\frac{h}{8\tau}+r-\iota)\delta_{i+1}^0+\int_{I_i^*}s(x,t_1), i=1,2,...,M-1.
\end{aligned}
\tag{22}
$$

Similarly, for $i=0$ and $i=M$ we have respectively

$$
\begin{aligned}
&(\frac{3h}{8\tau}+3r+\iota)\delta_0^1+(\frac{h}{8\tau}+r-\iota)\delta_1^1+\frac{h}{24}\{(7(\delta^2)_0^1+(\delta^2)_1^1\}\\
&=(\frac{3h}{8\tau}+3r+\iota)\delta_0^0+(\frac{h}{8\tau}+r-\iota)\delta_1^0+\int_{I_0^*}s(x,t_1),
\end{aligned}
\tag{23}
$$

$$
\begin{aligned}
&(\frac{h}{8\tau}+r-\iota)\delta_{M-1}^1+(\frac{3h}{8\tau}+3r+\iota)\delta_M^1+\frac{h}{24}\{(\delta^2)_{M-1}^1+7(\delta^2)_M^1\}\\
&=(\frac{h}{8\tau}+r-\iota)\delta_{M-1}^0+(\frac{3h}{8\tau}+3r+\iota)\delta_M^0+\int_{I_M^*}s(x,t_1).
\end{aligned}
\tag{24}
$$

Afterwards, the nonlinear system of equations is obtained as a complete discrete formula, which we can see below

$$
\begin{cases}
(\frac{3h}{8\tau}+3r+\iota)\delta_0^1+(\frac{h}{8\tau}+r-\iota)\delta_1^1+\frac{h}{24}\{(7(\delta^2)_0^1+(\delta^2)_1^1\}\\
=(\frac{3h}{8\tau}+3r+\iota)\delta_0^0+(\frac{h}{8\tau}+r-\iota)\delta_1^0+\int_{I_0^*}s(x,t_1), \qquad i=0,\\
(\frac{h}{8\tau}+r-\iota)\delta_{i-1}^1+(\frac{6h}{8\tau}+6r+2\iota)\delta_i^1+(\frac{h}{8\tau}+r-\iota)\delta_{i+1}^1\\
+\frac{h}{24}\{(\delta^2)_{i-1}^1+14(\delta^2)_i^1+(\delta^2)_{i+1}^1\}\\
=(\frac{h}{8\tau}+r-\iota)\delta_{i-1}^0+(\frac{6h}{8\tau}+6r+2\iota)\delta_i^0+(\frac{h}{8\tau}+r-\iota)\delta_{i+1}^0\\
+\int_{I_i^*}s(x,t_1), \quad i=1,2,...,M-1,\\
(\frac{h}{8\tau}+r-\iota)\delta_{M-1}^1+(\frac{3h}{8\tau}+3r+\iota)\delta_M^1+\frac{h}{24}\{(\delta^2)_{M-1}^1+7(\delta^2)_M^1\}\\
=(\frac{h}{8\tau}+r-\iota)\delta_{M-1}^0+(\frac{3h}{8\tau}+3r+\iota)\delta_M^0+\int_{I_M^*}s(x,t_1), \qquad i=M.
\end{cases}
\tag{25}
$$

We can iteratively solve the system (25) by using Newton iteration method for the nonlinear systems. To begin, we must calculate the initial value δ^0 with the help of the initial condition of the equation (1). Afterwards, we will be capable of determining the approximate solution at new time levels by using the time-dependent parameters δ^1 which are computed from (25).

By rearranging the equation (21) and $\lambda = \frac{\tau^{-\vartheta}}{\Gamma(2-\vartheta)}$ we have

$$\begin{aligned}
&(\frac{h}{8\tau} + (\beta + \frac{2}{h})\lambda)\delta_{i-1}^{k+1} + (\frac{6h}{8\tau} + (6\beta + \frac{8}{h})\lambda)\delta_i^{k+1} + (\frac{h}{8\tau} + \beta\lambda)\delta_{i+1}^{k+1} \\
&+ \frac{h}{24}\{(\delta^2)_{i-1}^{k+1} + 14(\delta^2)_i^{k+1} + (\delta^2)_{i+1}^{k+1}\} \\
&= (\frac{h}{8\tau} + (\beta + \frac{2}{h})\lambda)\delta_{i-1}^{k} + (\frac{6h}{8\tau} + +(6\beta + \frac{8}{h})\lambda)\delta_i^{k} + (\frac{h}{8\tau} + \beta\lambda)\delta_{i+1}^{k} \\
&+ \lambda\sum_{s=1}^{k}\Theta_s\{\beta[\delta_{i-1}^{k-s+1} - \delta_{i-1}^{k-s}] + (6\beta + \frac{8}{h})[\delta_i^{k-s+1} - \delta_i^{k-s}] + \beta[\delta_{i+1}^{k-s+1} - \delta_{i+1}^{k-s}]\} \\
&+ \int_{I_i^*} s(x, t_{k+1}),
\end{aligned} \tag{26}$$

where $\beta = \frac{h^2-8}{8h}$.

For $k > 0$ we have

$$\begin{aligned}
&(\frac{h}{8\tau} + (\beta + \frac{2}{h})\lambda)\delta_{i-1}^{k+1} + (\frac{6h}{8\tau} + (6\beta + \frac{8}{h})\lambda)\delta_i^{k+1} + (\frac{h}{8\tau} + \beta\lambda)\delta_{i+1}^{k+1} \\
&+ \frac{h}{24}\{(\delta^2)_{i-1}^{k+1} + 14(\delta^2)_i^{k+1} + (\delta^2)_{i+1}^{k+1}\} \\
&= (\frac{h}{8\tau} + (\frac{2}{h} + \beta(1 + \Theta_1))\lambda)\delta_{i-1}^{k} + (\frac{6h}{8\tau} + (6\beta + \frac{8}{h} + \Theta_1\beta)\lambda)\delta_i^{k} \\
&+ (\frac{h}{8\tau} + \lambda\beta(1 + \Theta_1))\delta_{i+1}^{k} \\
&- \lambda\sum_{s=2}^{k}(\Theta_{s-1} - \Theta_s)(\beta\delta_{i-1}^{k-s+1} + (6\beta + \frac{8}{h}))\delta_i^{k-s+1} + \beta\delta_{i+1}^{k-s+1}) \\
&- \lambda\Theta_k((\beta\delta_{i-1}^{0} + (6\beta + \frac{8}{h}))\delta_i^{0} + \beta\delta_{i+1}^{0}) + \int_{I_i^*} s(x, t_{k+1}).
\end{aligned} \tag{27}$$

3. Stability analysis

Now the Von-Neumann stability analysis [10] and mathematical induction can be used to investigate the stability conditions of the numerical method at hand.

Theorem 3.1. *The numerical scheme* (21) *to solve the initial and boundary value problem* (1) *is unconditionally stable.*

Proof. To investigate the stability conditions of the present numerical method, we use the Von-Neumann stability analysis and mathematical induction. First of all, the nonlinear term u^2 is linearized by taking the solution σ as a constant and, after that, we let $s(x,t) = 0$. As the error of the method has only to do with the time parameters δ_m^k, denoting $e^k := \delta^{k+1} - \delta^k$ as the error of scheme at time level k, we can rewrite the numerical scheme (21) as

$$
\begin{aligned}
&(\frac{h}{8\tau}+r-\iota+\frac{h\sigma}{24})\delta_{m-1}^{k+1}+(\frac{6h}{8\tau}+6r+2\iota+\frac{14h\sigma}{24})\delta_m^{k+1}+(\frac{h}{8\tau}+r-\iota\frac{h\sigma}{24})\delta_{m+1}^{k+1} \\
&= (\frac{h}{8\tau}+r-\iota)\delta_{m-1}^{k} + (\frac{6h}{8\tau}+6r+2\iota)\delta_m^k + (\frac{h}{8\tau}+r-\iota)\delta_{m+1}^k \\
&+ r\sum_{s=1}^{k}\Theta_s\{[\delta_{m-1}^{k-s+1}-\delta_{m-1}^{k-s}] + 6[\delta_m^{k-s+1}-\delta_m^{k-s}] + [\delta_{m+1}^{k-s+1}-\delta_{m+1}^{k-s}]\} \\
&- \iota\sum_{s=1}^{k}\Theta_s\{[\delta_{m-1}^{k-s+1}-\delta_{m-1}^{k-s}] - 2[\delta_m^{k-s+1}-\delta_m^{k-s}] + [\delta_{m+1}^{k-s+1}-\delta_{m+1}^{k-s}]\}.
\end{aligned} \tag{28}
$$

By definition $a = (\frac{6h}{8\tau}+6r+2\iota+\frac{14h\sigma}{24})$, $b = (\frac{h}{8\tau}+r-\iota+\frac{h\sigma}{24})$ and $c = (\frac{h}{8\tau}+r-\iota+\frac{h\sigma}{24})$, $d = (6r-2\iota)$, $e = (r-\iota)$ and $f = (r-\iota)$ the system of (28) can be converted into the matrix form as follows

$$
\mathbf{T}\delta^{k+1} = \mathbf{U}[\Theta_k\delta^0 + \sum_{s=0}^{k-1}(\Theta_s - \Theta_{s+1})\delta^{k-s}], \tag{29}
$$

where

$$
\mathbf{T} = \begin{pmatrix}
a & c & & & & & \\
b & a & c & & & & \\
 & b & a & c & & & \\
 & & \ddots & \ddots & \ddots & & \\
 & & & b & a & c & \\
 & & & & b & a & c \\
 & & & & & b & a
\end{pmatrix}, \mathbf{U} = \begin{pmatrix}
d & f & & & & & \\
e & d & f & & & & \\
 & e & d & f & & & \\
 & & \ddots & \ddots & \ddots & & \\
 & & & e & d & f & \\
 & & & & e & d & f \\
 & & & & & e & d
\end{pmatrix}.
$$

Then substituting the Fourier mode $e_m^k = v^k e^{im\rho}$ ($i := \sqrt{-1}$) into (28). We have

$$
\begin{aligned}
&v^{k+1}\{(\frac{h}{8\tau}+r-\iota+\frac{h\sigma}{24})e^{-i\rho} + (\frac{6h}{8\tau}+6r+2\iota+\frac{14h\sigma}{24}) + (\frac{h}{8\tau}+r-\iota+\frac{h\sigma}{24})e^{i\rho}\} \\
&= v^k\{(r-\iota)e^{-i\rho} + (6r-2\iota) + (r-\iota)e^{i\rho}\} \\
&+ \sum_{s=1}^{k-1}\Theta_s\{(v^{k-j+1}-v^{k-j}) \times ((r-\iota)e^{-i\rho} + (6r-2\iota) + (r-\iota)e^{i\rho}),
\end{aligned}
$$

or

$$
v^{k+1} = Q\{\Theta_k v^0 + \sum_{s=0}^{k-1}(\Theta_s - \Theta_{s+1})v^{k-s}\}, \tag{30}
$$

where

$$Q=\frac{2\alpha\cos\rho+\beta}{(2\alpha+\frac{h\sigma}{24})\cos\rho+(\beta+\frac{14h\sigma}{24})},$$

where $\alpha=\frac{h}{8\tau}+r-\iota$ and $\beta=\frac{6h}{8\tau}+6r+2\iota$.

It can easily be verified that

$$|Q|^2\le 1.$$

As a result, for $k=0$, (21) gives the following form:

$$v^1=Q\Theta_0 v^0,$$

and then

$$|v^1|=|Q||\Theta_0||v^0|\le|v^0|.$$

Let $|v^j|\le|v^0|$, $j=1,2,...,k$. Hence, by equation (30) we have,

$$\begin{aligned}|v^{k+1}|&\le\Theta_k|v^0|+\sum_{s=0}^{k-1}(\Theta_s-\Theta_{s+1})|v^{k-s}|\\&\le\Theta_k|v^0|+\sum_{s=0}^{k-1}(\Theta_s-\Theta_{s+1})|v^0|\\&=|v^0|(\Theta_k+\sum_{s=0}^{k-1}(\Theta_s-\Theta_{s+1}))\\&=|v^0|.\end{aligned}$$

Thus, for every k, we have $|v^{k+1}|\le|v^0|$. This relation demonstrates that $|e^{k+1}|\le|e^0|$, i.e., the error of this method in time level k, for every k, does not grow and is either less than or equal to its initial error. So, the unconditional stability of the method is verified. □

4. Numerical examples

In this section, we try to demonstrate, with some examples, that the numerical solution is the agreement to the theoretical analysis. We can measure the precision of the numerical method by both the L_2 error norm and the L_∞ error norm, where

$$\|u^{exact}-u_h\|_2^2\simeq h\sum_{j=0}^{N}|(u^{exact})_j-(u_h)_j|^2,$$

and

$$\|u^{exact}-u_h\|_\infty\simeq\max_j|(u^{exact})_j-(u_h)_j|.$$

All computations were conducted with the help of MATLAB software.

Example 1. Considering the following the fractional initial and boundary value problem below

$$\begin{cases} u_t + {}_0^C D_t^{\vartheta} u(x,t) - {}_0^C D_t^{\vartheta} u_{xx}(x,t) + f(u) = s(x,t), & \text{in } I \times (0,T], \\ u(0,t) = u(1,t) = 0, & t \in (0,T], \\ u(x,0) = 0, & \text{in } I, \end{cases} \tag{31}$$

with $I = (0,1)$ and $0 < \vartheta < 1$, where $s(x,t) = x(1-x) + \frac{t^{1-\vartheta}}{\Gamma(2-\vartheta)}(x(1-x)+2) + t^2x^2(1-x)^2$ and the exact solution is $u(x,t) = tx(1-x)$.

For the time and space stepsize sufficiently small, Table 2 and Table 3 show the numerical errors at $\vartheta = 0.05$ and $\vartheta = 0.95$ between the numerical solution and the exact solutions in time t_1. We denote that in Table 2, $\tau = 0.001$ and in Table 3, $h = 0.001$.

Table 2: Error of approximate solutions in $\tau = 0.001$, $h_i = \frac{1}{2^{i+1}}$ and $\vartheta = 0.05$ in t_1.

i	h	L_2-norm	L_∞-norm
1	0.25	0.00494547	0.00344572
2	0.125	0.00081220	0.00057444
3	0.0625	0.000124167	0.00008648
4	0.03125	0.00002070	0.00001312
5	0.015625	0.00000374	0.00000195

Table 3: Error of approximate solutions in $h = 0.001$, $\tau_i = \frac{1}{2^i}$ and $\vartheta = 0.95$ in t_1.

i	τ	L_2-norm	L_∞-norm
1	0.5	0.00437715	0.00019922
2	0.25	0.00056749	0.00002583
3	0.125	0.00022010	0.00010014
4	0.0625	0.00002842	0.00000129
5	0.03125	0.00000368	0.00000016

In Table 2, errors of approximate solutions in L_2-norm and L_∞-norm at $\tau = 0.001$, $h_i = \frac{1}{2^{i+1}}$ and $\vartheta = 0.05$ are presented.

Also, in Table 3, errors of approximate solutions in L_2-norm and L_∞-norm at $h = 0.001$, $\tau_i = \frac{1}{2^i}$ and $\vartheta = 0.95$ are presented.

Table 2 compares the analytical solution and numerical solutions obtained for $\vartheta = 0.05$ different number of divisions of the region. Obviously, there is harmony between the analytical and numerical solutions obtained by the present scheme. As the value of M increases, the values of error norms L_2 and L_∞ decrease. Table

3 illustrates the error norms L_2 and L_∞ for $\vartheta = 0.95$ at different time steps. Table 3 demonstrates that there is a correspondence between the decrease in the time steps, on the one hand, and the higher accuracy of the obtained numerical results, on the other. This can be seen from the decreasing values of the error norms L_2 and L_∞.

Figure 1 depicts the numerical solutions of Eq. (1) at the interval (0,1) for $\vartheta = 0.95$ and various values of M, n. We can see striking similarities in the graphs of the numerical and analytical solutions.

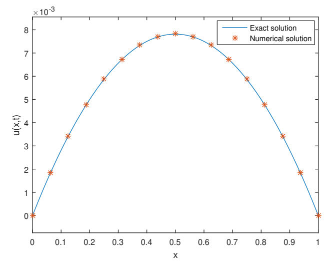

(a) $n = 32$ and $M = 16$ for t_1

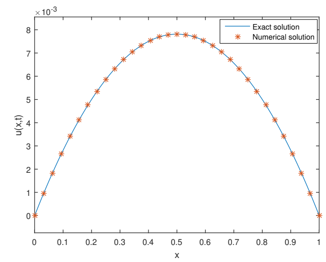

(b) $n = 32$ and $M = 32$ for t_1

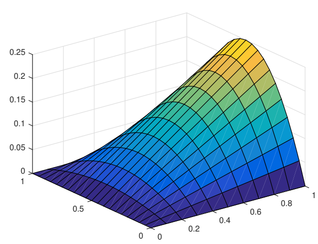

(c) $n = 10$ and $M = 20$ for all t

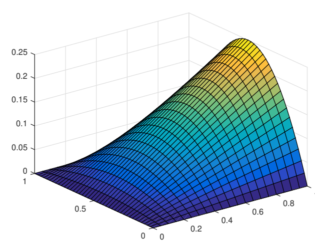

(d) $n = 20$ and $M = 40$ for all t

Figure 1: Numerical solutions of (31) in Example 1 for $\vartheta = 0.95$.

Example 2. As the second example, consider the nonhomogeneous fractional Cable equation (31) with

$$s(x,t) = [(1 + (1 + 4\pi^2)\frac{t^{1-\vartheta}}{\Gamma(2-\vartheta)} + \sin(2\pi x)] \sin(2\pi x)$$

and the exact solution is $u(x,t) = t\sin(2\pi x)$.

We can observe, in Table 4, the numerical errors at $\vartheta = 0.5$ for several h and τ.

Table 4 represents errors of approximate solutions in L_2-norm and L_∞-norm at $h = \tau_i = \frac{1}{2^{i+1}}$ and $\vartheta = 0.5$.

At this stage, we need to compare the results. Table 4 shows the comparison made for $\vartheta = 0.5$ and various mesh sizes and time steps. Obviously, there exists a good agreement between the solutions. An increase in M and n results in a

Table 4: Comparison of errors of approximate solution at $\tau_i = h_i = \frac{1}{2^{i+1}}$ and $\vartheta = 0.5$ in t_1.

i	$\tau = h$	L_2-norm	L_∞-norm
1	0.25	0.0563156	0.0435957
2	0.125	0.0113709	0.0069766
3	0.0625	0.0033776	0.0017897
4	0.03125	0.0026571	0.0008616
5	0.015625	0.0024747	0.0005352

decrease in L_2 and L_∞. The decrease in the error norms shows the accuracy of the newly obtained results. The accuracy of the newly obtained results can be shown by the decrease in the error norms. Finally, in Figure 2 we manifest the numerical solutions of Example 1 at the interval (0,1) for $\vartheta = 0.5$. Clearly, their graphs show a lot of similarities to each other.

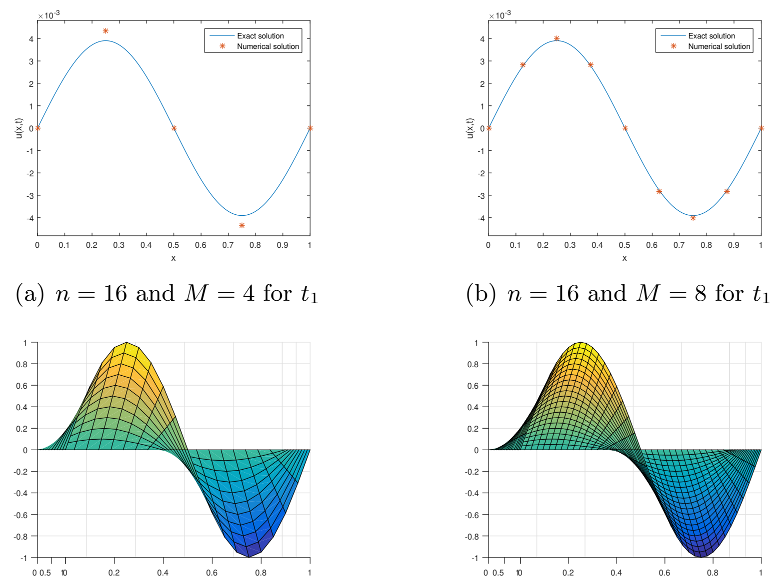

(a) $n = 16$ and $M = 4$ for t_1

(b) $n = 16$ and $M = 8$ for t_1

(c) $n = 4$ and $M = 16$ for all t

(d) $n = 8$ and $M = 16$ for all t

Figure 2: Numerical solutions of (31) in Example 2 for $\vartheta = 0.05$.

5. Conclusions

In the paper under study, we see how we can apply a numerical scheme based on finite volume element method to solve a class of nonlinear time-fractional Cable equation with initial and boundary condition. At the beginning, we utilize the finite volume element method and Newton's iterative algorithm in order to approximate the numerical solutions of the initial and boundary value problem. While doing this, the backward Euler method is employed to obtain the fully discrete form of the problem. Then we present the stability of the scheme at hand and, in the end, include some numerical results in order to demonstrate the scheme's applicability.

References

[1] M. Badr, A. Yazdani, H. Jafari, *Stability of a finite volume element method for the time-fractional advection-diffusion equation*, Numer. Methods Partial Differential Eq., 1459-1471.

[2] Y. Zheng, Z. Zhao, *The discontinuous Galerkin finite element method for fractional cable equation,* Applied Numerical Mathematics, 115 (2017), 32-41.

[3] Y. Wang, Y. Liu, H. Li, J. Wang, *Finite element method combined with second-order time discrete scheme for nonlinear fractional Cable equation*, The European Physical Journal Plus, 2016.

[4] Y. Lin, J. Lio, M. Yang, *Finite volume element methods: An overview on recent developments,* International Journal Of Numerical Analysis And Modeling, 4 (2013), 14-34.

[5] F. Lio, P. Zhuang, V. Anh, I. Turner, K., *Stability and conergence of the difference methods for the space-time fractional advection-diffusion equation,* Applied Mathematics and Computation, 191 (2007), 12-20.

[6] I. Podlubny, *Fractional differential equations*, Academic Press, New York, 1999.

[7] P. Zhuang, F. Liu, I. Turner, V. Anh, *Galerkin finite element method and error analysis for the fractional cable equation*, Numer. Algor., 72 (2015), 447-466.

[8] J. Liu, H. Li, Y. Liu, *A new fully discrete finite difference/element approximation for fractional cable equation*, Journal of Applied Mathematics and Computing, 52 (2015), 345–361.

[9] Y. Liu, Y. Du, H. Li, *A two-grid finite element approximation for a nonlinear time-fractional Cable equation*, Nonlinear Dynamics, 85 (2016), 2535–2548.

[10] S.B. Yuste, L. Acedo, *An explicit finite difference method and a new Von Neumann-type stability analysis for fractional diffusion equations,* Siam J. Numer. Anal., 42 (2005), 1862-1874.

[11] P. Zhuang, F. Lio, *Implicit difference approximation for the time fractional diffusion equation*, Journal of Applied Mathematics and Computing, 22 (2006), 87-99.

Accepted: December 18, 2019